PIV Measurements of the Spanwise Flow Characteristics
in a Naturally Transitioning Natural Convection Boundary Layer

Yongling Zhao, Chengwang Lei and John C. Patterson

School of Civil Engineering
The University of Sydney, Sydney, NSW 2006, Australia

Abstract

This paper presents particle image velocimetry (PIV) measurements of the spanwise flow characteristics in a natural convection boundary layer undergoing natural transition (i.e. induced by stochastic environmental disturbances). The boundary layer measured in the present experiment is formed adjacent to an isothermally heated plate immersed in water. The transition of the boundary layer from a transitional flow to a three-dimensional flow is visualised from the streamwise development of the spanwise flow structures. The frequencies and spatial wavenumbers of the spanwise flow structures at various streamwise positions are quantified by applying a two-dimensional Fourier transform to the time series of the spanwise velocity components measured along the spanwise direction. It is also understood that during the natural transition, spanwise flow structures appear in the boundary layer, which present a distinct frequency and a spatial wavenumber.

Introduction

Transition of boundary layers has been a continuing research topic for the fluid mechanics community for decades. Natural transition and controlled transition of boundary layers are the two main streams investigated extensively, with the natural transition referring to the transition induced by stochastic environmental disturbances and the controlled transition referring to the transition induced by specific artificial disturbances. Whilst controlled transition of Blasius boundary layers has attracted enormous research interest, natural transition of natural convection boundary layers has received little attention.

The pioneering investigations into the transition of natural convection boundary layers were reported in [1] and [2]. In both investigations a vibrating ribbon was used to introduce perturbations into the boundary layers. This type of perturbation mechanism was similar to that adopted in the classic experiment performed by Klebanoff et al. [3], in which the transition of Blasius boundary layers was studied. The transition studied by Klebanoff et al. [3] has been named K-type transition in Klebanoff's name. Similarly, the transition of natural convection boundary layers investigated by Jaluria and Gebhart [2] may be classified into one of the controlled transitions, that is the K-type transition or a K-type-like transition, rather than natural transition.

In the present study the natural transition of the natural convection boundary layers is investigated by visualising the spanwise flow structures at various streamwise positions. The frequencies and spatial wavenumbers of the spanwise flow structures at various streamwise positions are quantified. To the best knowledge of the authors, these are the first PIV measurements of the characteristics of natural convection boundary layers undergoing natural transition.

Experimental Setup and Methods

The experimental rig and the setup of the PIV system are shown schematically in figure 1. The stainless steel plate immersed in water has dimensions of 3mm (x) × 600mm (y) × 250mm (z), and is heated by circulating water between the Julabo water bath and the water jacket integrated to the back of the stainless steel plate. The Perspex tank is of 500mm×500mm×1000mm. The upper region of the tank, that is the region above the stainless steel plate, is designed as a buffer region for storing the heated water discharged from the boundary layer adjacent to the heated plate so that a non-stratified interior is maintained in the lower part of the tank for a sufficiently long time period to enable measurements to be taken in the quasi-steady stage of the boundary layer.
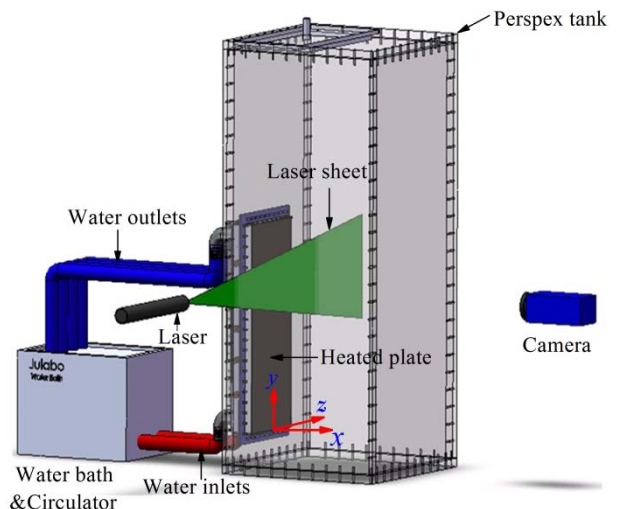

Figure 1. The experimental rig and setup of the PIV system.

For the measurement of the velocity field, a Lavision two-dimensional PIV system is used. The PIV system consists of a double-pulse Nd:YAG (Neodymiumdoped:Yttrium Aluminium Garnet) laser, a imager (camera) SX with a spatial resolution up to 4 Mega pixels, a programmable timing unit and particle image processing software.

In the present experiment, the camera is positioned 130 mm from the laser sheet and the focal length f of the camera is 201 mm. The field of view (FOV) is 140 mm×110 mm, with a resolution of 2800 pixels × 2200 pixels. The FOV covers a width of -70 mm$\leq z \leq$70 mm in the spanwise direction and the region ranging from y=330 mm to y=440 mm in the streamwise direction parallel to the heated plate. (The origin of the adopted Cartesian coordinate system is located at the mid-span of the leading edge of the plate, but is 10 mm off the plate in the x-direction, as shown in figure 1). The water in the Perspex tank is seeded with

20 μm polyamide particles, which have a specific gravity of 1.03. To achieve approximately 5-10 particles per interrogation window, 8 g of particles are added to the 250 L of water in the tank. In order to position the laser sheet precisely in the x-direction, a manual XY stage plus rotation platform (MAXYR-125L, Optics Focus Solution) is used to mount the laser head so that the distance between the laser sheet and the heated wall can be adjusted to an accuracy of 0.03mm. In the present experiment, the distance between the laser sheet and the heated wall is fixed a 10 mm.

The recording of particle images employs a single-frame mode because the flow velocity to be measured is very slow. The exposure time of the camera is set to 2000 μs and the recording rate is 15 Hz. Before the measurement starts, the seeded water has settled for about 3 hours after stirring. The initial temperature of the quiescent water in the Perspex tank is 23.0ºC and the heating temperature is set to 33.0ºC. The measurement takes 6300 particle images (i.e. over a period of 7 minutes). To record the velocity field of the residual flow, the PIV recording starts at about 25 seconds before the heating of the plate starts.

Results and Discussions

To ensure the subsequent analyses are performed in the quasi-steady stage of the boundary-layer flow, the overall development of the boundary layer is firstly examined.

Figure 1 shows the time series of the spanwise velocity component measured at a representative position (y=375 mm and z=0) within the FOV. It is seen in this figure that the time series of the spanwise velocity can be broadly divided into three stages, which are the residual flow stage (I), the start-up flow stage (II) and the quasi-steady stage (III). In the residual flow stage, the spanwise velocity is zero with no fluctuation, which suggests that the flow field is quiescent. When the heating of the plate starts, the spanwise velocity starts to oscillate more and more dramatically. The strong oscillations over the time period 50~100 seconds are due to the perturbations associated with the start-up of the system (e.g. the vibration caused by the circulator) and the leading edge effect of the boundary layer. It is worth noting the large oscillation that appears approximately 30 seconds after the initiation of heating, which corresponds to the travelling of the perturbation from the leading edge of the plate to the measuring position. With the decay of the start-up perturbations and the passage of the leading edge effect, the spanwise velocity returns to a state of oscillation at relatively small amplitudes, indicating a quasi-steady stage of the boundary layer (i.e. stage III). It is worth noting that the three stages shown in figure 2 are indicative only, and the present study is mainly concerned with the flow characteristics in the quasi-steady stage. The subsequent analyses are carried out with the experimental data over the time period of 200-350 seconds.
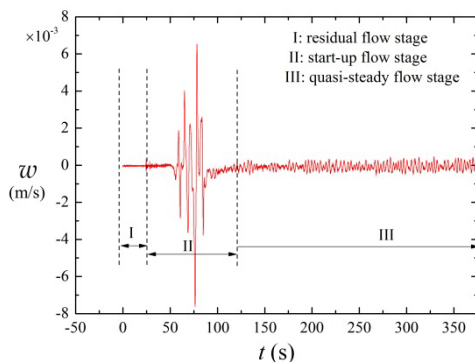

Figure 2. Time series of the spanwise velocity components measured at a representative position (y=375 mm and z=0) in the field of interest, indicating the three stages of the development of the boundary layer.

To verify the present measurement, the frequency of the boundary layer under investigation is compared against the theoretically predicted value of the boundary layer, which is shown in figure 3. The frequency in the experiment is obtained by performing a fast Fourier transform of the time series of the streamwise velocity component measured in the quasi-steady stage of the boundary layer. The theoretical frequency of the boundary layer is estimated using equation (3.2) in [4]. It is worth noting that the frequency estimated using this equation is in a non-dimensional form, which has been converted to a dimensional value so that the comparison can be made with the present experimental result. It is seen in figure 3 that the frequency of the boundary layer obtained from the present PIV experiment is approximately 0.31 Hz, which is comparable to the theoretical frequency of 0.33 Hz, as indicated by the dashed line. It is worth clarifying that the correlation given in [4] for the estimation of the frequency of thermal boundary layers was obtained based on the studies of two-dimensional boundary layers. However, as will be shown below, the boundary layer investigated in the present experiment has approached a three-dimensional flow stage at the streamwise position y=375 mm. The good agreement seen in figure 3 suggests that the boundary layer under investigation is in a weak three-dimensional regime, in which the frequency of the boundary layer has not been significantly affected by the three-dimensional flow structures.
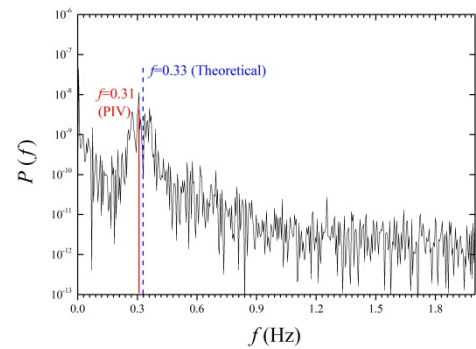

Figure 3. Power spectrum of the streamwise velocity components of the transitional flow stage. The dashed vertical line indicates the theoretical characteristic frequency of the flow.

Prior to the visualising of the spanwise flow structures of the boundary layer in the quasi-steady stage, the residual flow on the same observation plane is examined to confirm that the residual flow is not significant in the experiment. The residual flow is shown in figure 4(a) and the quasi-steady flow is shown in figure 4(b). It is clear in figure 4(a) that the residual flow is insignificant. The discrete small packets of non-zero spanwise velocities are due to environmental noise in the experiment. In the quasi-steady stage, it is clear that the spanwise flow structures are distinct and align well in both the spanwise and the streamwise directions, as shown in figure 4(b). It is worth noting that the same scale of the spanwise velocity is used in figures 4(a) and (b) to facilitate the comparison. The spanwise flow structures shown in figure 4(b) are observed at a time instant in the quasi-steady stage of the boundary layer. In order to understand the temporal and spatial evolutions of the spanwise flow structures in the transitioning boundary layer, the time series of the spanwise velocity measured along the spanwise direction at various streamwise positions within the thermal boundary layer are examined.
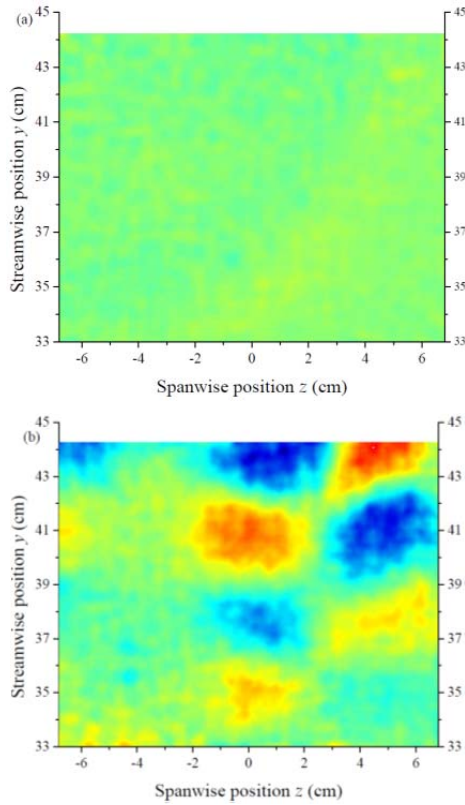
Figure 4. Contours of instantaneous spanwise velocity in (a) the residual flow stage and (b)the quasi-steady flow stage (red and blue show the maximum (+0.001 m/s) and minimum value (-0.001 m/s), respectively).

Figure 5 shows the temporal development of the spanwise velocity measured along the spanwise direction at three streamwise positions. The streamwise positions are measured from the leading edge of the heated plate, which are given in the caption of figure 5.

It is seen in figure 5(a) that, at this streamwise position, the spanwise flow structure is not distinct, whereas slightly twisted spanwise stripes appear in time, which suggests that the flow just transits into a weak three-dimensional regime from a two-dimensional regime. The alternate appearance of the stripes is due to the passage of two-dimensional travelling waves. It is expected that in a complete two-dimensional regime straight spanwise stripes, rather than twisted strips, would appear in time. However, due to the size limitation of the FOV, such a complete two-dimensional regime was not covered in the present measurement. The local Rayleigh number corresponding to this streamwise position (y=333.4 mm) for figure 5(a) is $Ra_L = 4.0 \times 10^9$, where Ra_L is the local Rayleigh number defined in terms of the distance from the leading edge of the heated wall to the position where the measurement is taken. The definition of Rayleigh number is the same as that adopted in [4].

At the downstream location of y=358.8 mm, spanwise flow structures start to manifest, as seen in figure 5(b). The flow structures shown in figure 5(b) indicate the existences of a temporal periodicity and a spatial wavenumber of the spanwise flow structures, though they are relatively weak. At the further downstream position of y=436.2 mm, corresponding to a local Rayleigh number $Ra_L = 9.0 \times 10^9$, the spanwise flow structures become more pronounced in both the spatial and temporal domains, as shown in figure 5(c). It is seen in this figure that the spanwise flow structures appear periodically in time and the spanwise wavelength of the flow structures remains approximately unchanged with time. It is worth clarifying that in

the present PIV experiment no artificial perturbations are introduced into the boundary layer. The transition of the boundary layer observed above is a result of its response to the stochastic environmental disturbances, which are believed to comprise of a wide band of competing frequencies, wavelengths and amplitudes. The transition is therefore recognised as the 'natural' transition of the boundary layer.
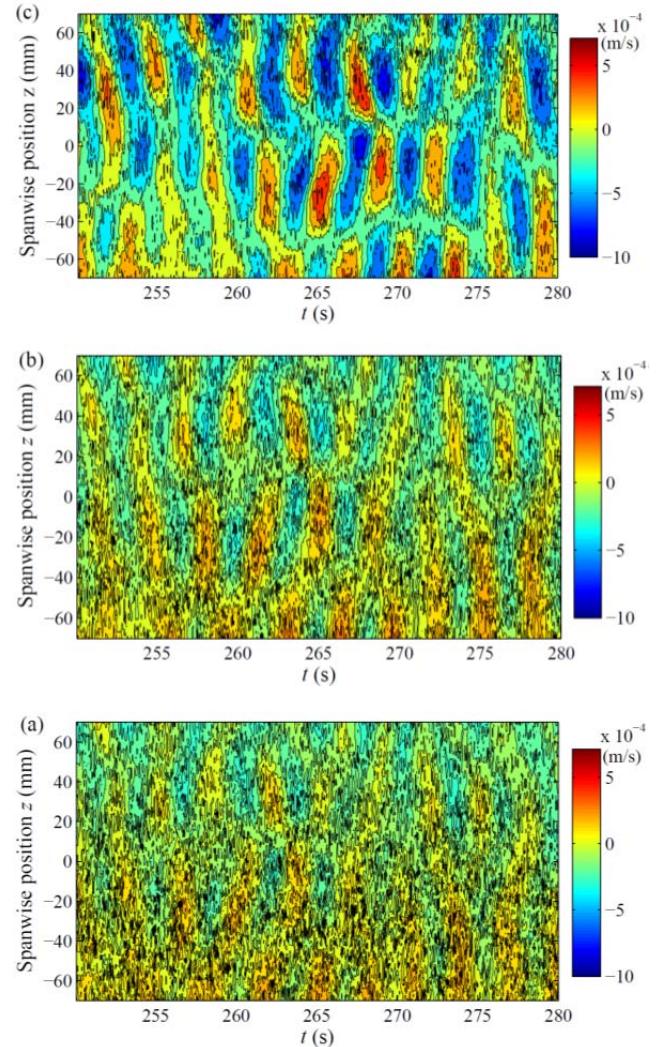

Figure 5. The temporal development of the spanwise velocity, measured along a spanwise direction at (a) y=333.4 mm (b) y=358.8 mm and (c) y=436.2 mm. The velocity scale for each plot is the same.

In order to quantify the temporal and the spatial development of the flow structures shown in figure 5, a two-dimensional Fourier transform is applied to the time series shown in figure 5 to obtain the frequency and the spatial wavenumber at each streamwise location. The results are presented in figure 6.

For the temporal evolution of the spanwise flow structures measured along the spanwise direction at y=333.4 mm, it is clear that two distinct peaks appear, indicating two dominant frequencies and two dominant spatial wavenumbers. The frequency and the spatial wavenumber of the spanwise flow structures are indicated by the peak pointed at by the solid (red) arrow. It is worth noting that the peak pointed by the dashed (blue) arrow is not relevant to the discussion here because the spanwise flow structures over the entire temporal domain are recognised as a flow cycle by the two-dimensional Fourier transform, which causes a false peak.

It is also worth clarifying that the frequency (*f*=0.322 Hz) of the spatial periodicity obtained here is slightly different from the frequency (*f*=0.31 Hz) obtained from the Fourier transform of the time series of velocity (see figure 3).This difference may be caused by the different ways adopted for obtaining these two frequencies. The former is obtained from the two-dimensional Fourier transform of flow properties, whereas the latter is obtained from the one-dimensional Fourier transform of the flow property measured within the boundary layer. Experimental noises in these two methods may contribute differently to the frequencies.
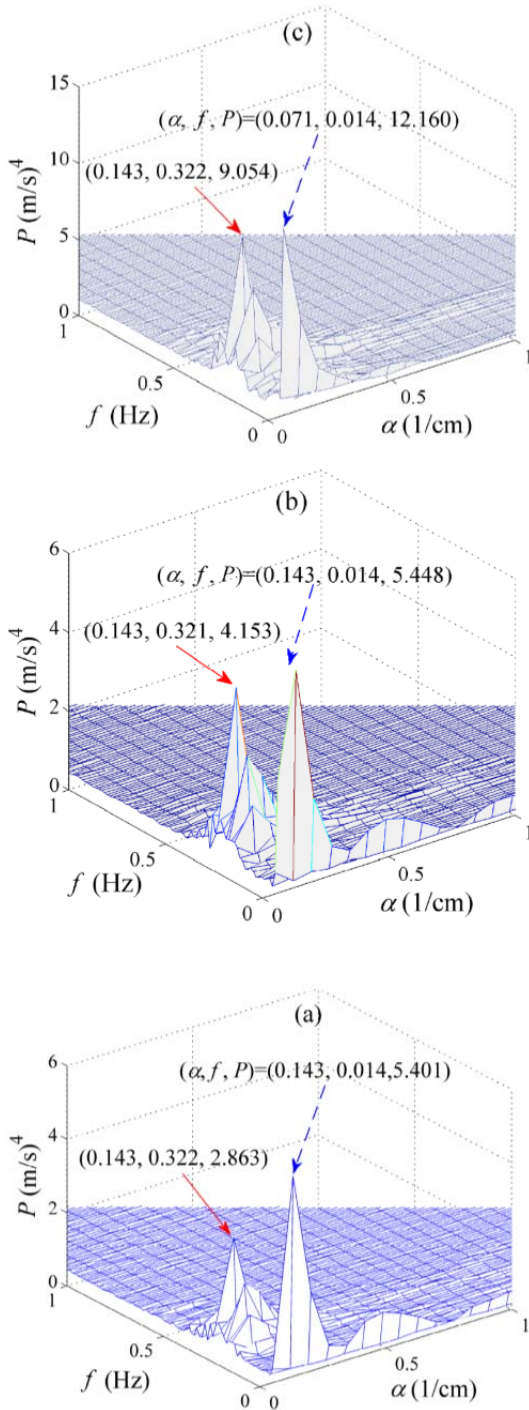

It is seen in figure 5(a) that these spanwise flow structures are extremely weak at the current location, as indicated by the power of the transform, which is several times less than the subsequent values for *y*=358.8 mm and *y*=436.2 mm (see below). The flow at this streamwise position is therefore recognised as a transitional flow, which is transiting from a two-dimensional regime to a three-dimensional regime.

Further downstream at *y*=358.8 mm (figure 6b), it is clear that there appears two distinct peaks, indicating two dominant frequencies and two spatial dominant wavenumbers. It is worth noting that the low-frequency peaks indicated by the dashed arrows in figures 6(b) and (c) are again false signals and not relevant to the discussion here. The frequency and the spatial wavenumber of the spanwise flow structures are indicated by the peak pointed at by the solid (red) arrow. At *y*=436.2mm (figure 6c), the same spatial wavenumber and a slightly varied frequency are obtained, as indicated by the solid (red) arrow. It is seen in figure 5(c) that these spanwise flow structures have become distinct and the flow at the current location is therefore recognised as a three-dimensional flow.

Conclusions

A PIV measurement of the velocity field within the natural convection boundary layer is performed on a plane parallel to the heated wall. The transition of the boundary layer from a transitional flow to a three-dimensional flow is visualised from the spanwise flow structures at various streamwise positions. The spanwise flow structures are also quantified. To obtain the frequency and the spatial wavenumber of the spanwise flow structures, a two-dimensional Fourier transform is applied to the time series of the spanwise velocity measured along the spanwise direction. It is now demonstrated that during the 'natural' transition of the natural convection boundary, spanwise flow structures appear in the boundary layer, which present a distinct frequency and a spatial wavenumber.

Acknowledgement

References

[1] Čolak-Antić, P. & Görtler, H., Flow visualization studies of free convection laminar-to-turbulent transition along a heated vertical plate in water induced by two-dimensional forced disturbances, Heat and Mass Transfer, 4, 1971, 25-31.

[2] Jaluria, Y. & Gebhart, B., An experimental study of nonlinear disturbance behaviour in natural convection, *J. Fluid Mech.*, **61**, 1973, 337-365.

[3] Klebanoff, P.S., Tidstrom, K.D., & Sargent, L.M., The three-dimensional nature of boundary-layer instability, *J. Fluid Mech.*, **12**, 1962, 1-34.

[4] Zhao, Y., Lei, C., & Patterson, J.C., Resonance of the thermal boundary layer adjacent to an isothermally heated vertical surface, *J. Fluid Mech.*, **724**, 2013, 305-336.

Figure 6. Two-dimensional Fourier transform of the spanwise velocity measured along a spanwise direction at various streamwise positions. (a) *y*=333.4 mm (b) *y*=358.8 mm and (c) *y*=436.2 mm. *f* and *α* are frequency and spatial wavenumber, respectively.